DE GRUYTER DOI 10.1515/jmbm-2012-0008 — J Mech Behav Mater 2012; 21(1-2): 3–20

Oscar Philander, Graeme John Oliver and Bohua Sun*

# Experimental and numerical investigation into the behavior of shape memory alloys

**Abstract:** Research and development of smart alignment systems is currently being undertaken at the Smart Devices and MEMS Laboratory at the Cape Peninsula University of Technology. The intended devices will harness the remarkable phenomena of shape memory alloys (SMAs), i.e. the shape memory effect and pseudo-elasticity, for actuation purposes. These unique characteristics of shape memory alloy behavior results from an austenitic ⇔ martensitic phase transformation during heating or cooling and/or a de-twinning of the martensitic variants due to an applied load. This paper investigates the microscopic and macroscopic behavior of SMA wires and uses the dynamic one-dimensional thermodynamic and statistical thermodynamic constitutive model proposed by Müller and Achenbach and further refined by Müller and Seelecke in the design of SMA line actuators. This model permits the simulation of the response of a tensile specimen to a thermodynamic input and calculates all phase transformations, phase proportions and deformations as functions of time if the temperature and applied load are prescribed as functions of time. The aim of this research is to develop an understanding of the numerical model and its implementation in the design of SMA line actuators. Specific results should show response time of a given length of SMA wire subjected to an applied load and temperature increase, and the load – displacement relationships for both quasi-plastic and pseudo-elastic behaviors. This paper also introduces some of the devices currently under investigation by the Smart Alignment Systems Research Group.

**Keywords:** intelligent structures; shape memory alloys; SMA line actuator; smart materials; statistical thermodynamics; thermodynamics.

***Corresponding author: Bohua Sun,** Department of Mechanical Engineering and Centre for Research in Applied Technology, Cape Peninsula University of Technology, P.O. Box 1906, Bellville 7535, Cape Town, South Africa, e-mail: sunb@cput.ac.za
**Oscar Philander:** Department of Mechanical Engineering and Centre for Research in Applied Technology, Cape Peninsula University of Technology, P.O. Box 1906, Bellville 7535, Cape Town, South Africa
**Graeme John Oliver:** Department of Mechanical Engineering and Centre for Research in Applied Technology, Cape Peninsula University of Technology, P.O. Box 1906, Bellville 7535, Cape Town, South Africa

## 1 Introduction

Engineers and technologist are called upon to develop a new generation of "smart" products that may be used in military, aerospace, medical, automotive, and commercial products for the 21st century. The development of these products has previously been accomplished through the advancement of smart materials and intelligent structures with inherent "brains", "nervous systems", and "skeletons". They were realized through the integration of knowledge bases associated with material science, information technology and biotechnology [1].

Numerous application of smart structures technology to various physical systems is evolving to actively control vibration, noise, damping, shape and stress distribution. Applications range from space systems, fixed-wing or rotary-wing aircraft, automotive, civil structures and machine tools. Much of the earlier development of smart structures methodology was driven by space applications such as vibration and shape control of large flexible space structures, but now wider applications are envisaged for aeronautical and other systems [2].

A smart structure incorporates sensors, actuators and processors to enable adaptation to changing operational and/or environmental conditions, thereby enhancing performance, stability, and/or safety. Advances made in smart materials have enabled smart structures [3]. Smart materials such as piezoelectric, magnetostrictive, shape memory alloys, etc; exhibit greater expansion/contraction in response to a controlling external stimuli (electric or magnetic field, thermal, chemical, etc.). Their metrics – energy density, specific work, and power density – are at least an order magnitude if not more than conventional technology (electromagnetics, hydraulics, pneumatics, etc.). Thus, more control authority can be delivered in less space with less weight [3].

When assessing a smart material for actuation the three main characteristics are force, stroke and frequency of response (speed). There is however, not one golden smart material that excels at all three; instead one or more of these are compromised and it differs between the various smart material phenomena. For example, Piezoelectrics are fast (up to MHz) and can deliver large forces, (kN) but the strokes are very small (microns). On the other hand, shape memory alloys can provide both large forces (100 to kN) and large displacements (mm to cm), but are inherently slow in response time (<8 Hz) [3].

Shape memory alloys fall within this realm of being termed “smart” in that they belong to a special group of metallic materials that remembers their shape even after severe deformation [4, 5]. When a load is applied to the material at low temperatures, it will deform causing an apparent plastic deformation, which is maintained until an increase in temperature causes the deformation to disappear completely. Four to 8% erasable deformations have been observed in alloys like NiTi, CuZnAl, CuAlNi, and AuCd. This material response is termed the shape memory effect [4, 6–11].

At high temperatures however, the material exhibits a material response termed the pseudo-elastic behavior, and plastic deformations are recovered by releasing the applied load [4, 6]. This high temperature material response is also characterized by significant internal damping, non-linear elastic ranges, non-homogeneous deformations and high yield stresses [4, 10, 11].

The unique material responses associated with shape memory alloys, i.e., the shape memory effect, and the pseudo-elastic effect are ascribed to shear deformations associated with a thermo-elastic martensitic transformation and its reverse transformation [12–14]. In a typical transformation during cooling, the high-temperature austenitic phase structure, which has a greater crystallographic symmetry than the low-temperature martensitic phase gives rise to the formation of multiple symmetry-related variants or proportions of twinned martensite when a critical temperature, the martensitic start temperature, $M_s$, is reached. Up to 24 different variants of martensite may result from this transformation, which is completed when the martensitic finish temperature, $M_f$, is reached [10]. This transformation however, does not cause the formation of locked in stresses as observed in classical steels, and hence no change in the geometric dimensions of the material occurs. These twinned variants of martensite form complex patterns at a length-scale much smaller than the size of the specimen. The actual length-scale can range from a few nanometers to tenths of millimeters and it depends on a variety of factors including the chemical composition, specimen size, grain size and heating and/or cooling history [12, 15–17].

When a load is applied to the material, while in the twinned martensitic state (at low temperature), only those variants of martensite sensitive to the applied load will transform through a process of de-twinning the twinned variants of martensite and cause an apparent macroscopic plastic deformation. An increase in temperature will transform this de-twinned martensitic crystal structure back to austenite and the material regains its original dimensions. This process is termed the shape memory effect. The critical temperature at which the de-twinned martensite transformed to austenite is the austenitic start temperature, $A_s$, and the temperature at which all the de-twinned martensite fully transforms to austenite is termed the austenitic finish temperature, $A_f$ [10, 16, 17, 19].

If a specimen is heated to a temperature between the $M_s$ and $A_f$ temperatures it may contain variants of twinned martensite, austenite or a mixture of the two. If a load is now applied to the material, it transforms to de-twinned martensite and produces an apparent plastic deformation as in the shape memory effect. Unloading results in either an elastic response or a partial reverse transformation to austenite that follows a hysteretic path, depending on the temperature being either above or below the $A_s$ temperature. The latter material response is also termed the partial pseudo-elastic effect. The remaining apparent plastic deformation can completely be recovered by heating above the $A_f$ temperature [15–17, 19].

When a load is applied to the high temperature austenitic phase (above the $A_f$ temperature), it will first perform elastically until a certain transformation or yielding value of stress is reached. The austenite will now transform to de-twinned variants of martensite and again induce an apparent macroscopic plastic deformation. This deformation is maintained until subsequent unloading forces the material to now follow a hysteretic unloading path and all deformation is removed. This process describes the pseudo-elastic behavior of the material.

The reverse transformations of the shape memory effect (upon heating) and the energy dissipation due to the hysteretic partial pseudo-elastic and pseudo-elastic behaviors produce actuation forces that could be harnessed for various actuator applications in mechanical systems. This has been the focus of researchers and inventors for the past 40 years [5]. For practical applications, shape memory alloys are usually used in NiTi alloy form [18, 19].

Kauffman and Mayo [20] while commissioned to develop a material for the nose cone of the US Navy missile, SUBROC, discovered this material in 1961. The goal of this work was to find a material that had a high melting point and high impact resistant properties and NiTi alloy best suited these criteria. It was only later through an accident that Beuler stumbled upon the remarkable shape memory characteristics of this material.

Since then NiTi alloy wires have be used in many novel applications ranging from shower springs that are activated above a certain temperature to shut off water that is too hot to the active shape control used in the adaptive aerodynamic lifting surface of a variable camber wing both utilizing the shape memory effect. Energy dissipation in pseudo-elastic hysteresis has successfully been used in vibration damping of mechanical systems [2, 5, 18, 21, 22].

The successful design of smart or intelligent structures with either embedded shape memory alloy fibers or structural shape memory alloy components relies on a good constitutive description for this material behavior [4, 19]. Literature shows us that this is indeed an enormous task in that the complicated coupling between mechanical and thermal properties and many aspects of their interactions as it pertains to the phase transformations occurring in this material has to be taken into account. This is evidenced by the sensitivity of the transformation temperature and other properties by relatively small changes in the composition of the alloy by various thermo-mechanical treatments and the effect of rate dependencies, which includes thermal and/or mechanical responses on transformation processes [4, 8, 24–26, 33].

## 1.1 Review of experimental analyses and findings on shape memory alloys

The above discussion shows that at the heart of the unique material responses that shape memory alloys exhibit lies within its austenite (A) ⇔ twinned martensite ($M^T$) transformation upon heating or cooling, the austenite (A) ⇔ de-twinned martensite ($M^{DT}$) transformation at elevated temperatures due to an induced stress (either tension, compression, torsion, etc.), and the twinned martensite ($M^T$) ⇒ de-twinned martensite ($M^{DT}$) transformation at low temperature due to an induced stress (either tension, compression, torsion, etc.). These phase transformations have been the focus of many experimental studies in the past 40 years [4, 8, 10, 11, 17, 27–31].

Otsuka et al., Delaey et al., Schetky, [14, 20, 31] were among the first researchers to report that the remarkable behavior of shape memory alloys is caused by an interplay of a high temperature austenite phase and a low temperature martensite phase. Furthermore, [4] demonstrated that the transformation temperature and other properties of shape memory alloys could be altered by small changes in the composition of the alloy and by various thermo-mechanical heat treatments. Daniels, and Pope and Judd used a differential scanning calorimeter to study the phase transformations exhibited by shape memory alloys [4].

For most practical engineering applications, shape memory alloys are usually used in NiTi alloy wire forms [18]. After the shape memory effect was first observed in NiTi alloys a great amount of metallurgical research has gone into it and Wasilewski, Jackson et al., Ling and Kaplow and Miyazaki were among the first researchers to experimentally study NiTi [4]. These experiments looked at the effects of temperature, strain range and mechanical cycling on NiTi alloys.

Due to the complexities of the energy dissipation associated with the hysteretic nature of pseudo-elastic behavior, most researchers appeared to study this phenomenon experimentally more than the shape memory effect. Wayman and Deurig, Wayman, and Fu are among these researchers while Müller and Xu, and Fu, Müller and Xu were among the first to experimentally study the interior of the hysteresis loop [32, 33, 39].

As time progressed and experimental apparatus became more sophisticated Chrysochoos et al., Shaw and Kyriakides, Tobushi et al. and Lim and McDowell found that the pseudo-elastic material response of shape memory alloys is associated with significant temperature variations. Furthermore, the stress-induced austenite (A) ⇔ de-twinned martensite ($M^{DT}$) transformation at elevated temperatures occurs in well-defined stress – temperature regions, it is dependant on the kind of mechanical-loading – unloading and thermal-heating – cooling cycles, and the combined effects of the mechanical and thermal cycles [4, 10, 11, 32].

The stress-induced austenite (A) ⇔ de-twinned martensite ($M^{DT}$) transformation at elevated temperatures is an unstable transformation and thus produces inhomogeneous macroscopic deformations as reported by Leo et al., Shaw and Kyriakides, Sittner et al. [4, 10, 11, 31, 32]. From a crystallographic point of view, the de-twinned martensite ($M^{DT}$) phase nucleates and grows as interfaces within the austenite phase until all the austenite has transformed to de-twinned martensite ($M^{DT}$). Larche and Cahn, Robin, Heidug and Lerner, Johnson and Alexander were among the first researchers to study the equilibrium conditions of these interfaces and motion of the interfaces between regions of two phases [33, 34]. Salzbrenner and Cohen performed investigations to study the motion of these interfaces by controlling the temperature [33, 34].

The type of loading cycle (tension, compression, torsion, etc.) to induce the austenite (A) ⇔ de-twinned martensite ($M^{DT}$) transformation at elevated temperatures, and the twinned martensite ($M^T$) ⇒ de-twinned martensite ($M^{DT}$) transformation at low temperature also has important implications to the shape memory alloy material response. Adler et al. and Melton showed experimentally that shape memory alloys subjected to compressive loading showed lower recoverable strains, steeper hardening behavior, and higher transformation stress levels compared to tensile behavior [19]. Leo et al., Shaw and Kyriakides, Sittner et al., Gall et al., and Zang et al. studied the effects of tension – compression asymmetry on shape memory material response [4, 10, 11, 31]. Gall and Sehitoglu performed experiments on one-dimensional shape memory alloy bars loaded in tension and compression. Their results showed that the shape memory alloy phase transformations is influenced by the texture of the specimen [19].

Sittner et al. performed experimental analyses to study the three-dimensional constitutive behavior of shape memory alloys. They investigated the stabilization of transformation behavior in stress-induced martensitic transformation in NiTi alloy hollow bar. The loading cycles were for combined Tension and Torsion. The specimen was then loaded either in tension or torsion. The results revealed strain anisotropy, which implies the existence of other strain components [31].

Jacobus et al. studied the effect of stress state on the stress – induced martensitic phase transformation. NiTi alloy bar specimens were subjected to tension, compression, hydrostatic pressure, and various tri-axial compression tests. The results showed that shape memory alloy phase transformation is pressure dependant and the effective stress for phase transformation increase with increasing hydrostatic pressure [19].

Lim and McDowell conducted experiments on shape memory alloy torque tubes using proportional and non-proportional loading conditions. They investigated the stress-temperature coupling in tension, compression, and torsion. Their results showed that more latent heat was available in compression, which was evidenced by larger temperature increases in compression than in tension for the completion of a phase transformation. They also found that the thermo-mechanical behavior in positive and negative torsion was found to be symmetrical [19].

In conclusion all experimental efforts tries to bridge the gap between the microscopic and macroscopic material responses of shape memory alloys. The experimental findings detailed above shows the strong coupling between thermal and mechanical properties of shape memory alloys. The mechanical material response is dependant on many factors including temperature, strain range, thermo-mechanical history, loading rate, specimen geometry, nature of ambient medium, and the interactions of some of these (see [4, 10]). Furthermore, the phase transformations associated with the shape memory effect and the pseudo-elastic effect produces unstable material behavior and inhomogeneous deformations due to the propagating phase transformation phenomena, which is also temperature and load dependant. Added to this is the sensitivity of the phase transformations on magnitude and type of the applied loading and unloading conditions. All of these material complexities make the constitutive modeling of shape memory alloys an enormous task. In order for successful constitutive models to be constructed knowledge bases associated with Material Science, Physics, Mathematics, and Engineering has to merge.

## 1.2 Review of constitutive modeling for shape memory alloys

Research related to the constitutive modeling of shape memory alloys have focussed on phenomenological and micro-mechanics approaches. Within these approaches their exist sub-groups such as state space phenomenological [35, 36], two- and three-component phenomenological [26], crystallographic micro-mechanics, free energy function micro-mechanics [19, 35] and micro-plane models [18]. Constitutive models following the state space phenomenological approach, has been the engineers choice since they are conceptually easy to implement and use measurable quantities as parameters in their construction. Most of these models were constructed to fit one-dimensional experimental data and thus predict the uniaxial mechanical behavior of these materials very well [35, 36]. They do however lack the thermodynamic aspects related to the shape memory alloy material response and their suitability for the simulation in actuator applications is very limited [36]. Micro-mechanics models on the other hand follow the crystallographic behavior of these materials quite well and although they possess a very high level of sophistication, they are far too complex for use in the design of one-dimensional shape memory actuators [36].

Other constitutive models based on the Maxwellian Visco-elastic approach [37], and the Rubber-like approach [38], are developed from experimental observations and an in depth knowledge of the mechanics of solid structures. These models, however, only show good qualitative agreement with experimental data [37, 38] and work still has to be conducted to bring them to a quantitative level.

This research focuses on the use of a constitutive description for shape memory alloys based on the multi-well approach [22, 33, 36, 39, 41]. This approach not only incorporates the complex thermodynamic and mechanical aspects of the shape memory alloy material behavior, but also lends itself to integration into robust numerical algorithms within a computational setting [23, 36, 39–41].

These factors make this constitutive model a prime candidate for use in the design of complex multi-dimensional structural engineering systems that uses one-dimensional shape memory alloy actuators for active and/or passive vibration control or active shape control applications. We will therefore not try to improve on any of the existing constitutive models, but rather employ the selected model to suit our experimental data through calibration and use it in the design of our smart shape memory alloy line actuators.

# 2 Experimental and macroscopic observations of quasi-plastic material response exhibited by shape memeory alloys

## 2.1 Introduction

In order to fix ideas about our present investigation into the complex constitutive modeling of shape memory alloys it is necessary to present some experimental data and results obtained for these materials. Shape memory alloys exhibit two unique material responses ascribed to solid-solid thermo-elastic martensitic forward and reverse phase transformations, i.e., the shape memory effect and the pseudo-elastic effect. The experimental investigation was performed to study only one aspect of the shape memory effect, the quasi-plastic material response under tensile loading conditions. Shape memory alloy while in its low temperature martensitic state exhibit this behavior under different loading conditions (tension, compression, torsion, tension-torsion, compression-torsion, etc.). The experimental results obtained are consistent with what other researchers found in the field and even show some interesting findings regarding this unique material response. It is hoped that these results will add to the body of work performed in this area of research but also more importantly provide an insight into the different approaches used in the constitutive modeling of shape memory alloys. All experiments were conducted at the Strength of Materials Laboratory of the Department of Mechanical Engineering at the Peninsula Technikon.

## 2.2 Materials tested

Commercially available NiTi shape memory alloy wires of 1, 2 and 3 mm diameter were used in these experiments. The material was obtained from the supplier Johnson Matthey (San Jose, CA, USA) and Table 1 shows their properties. It should be noted that quantitative comparison of these three materials would not be possible since slight changes in the chemical composition may result in drastic inconsistencies with regards to material responses. We will therefore have a qualitative discussion on the material response of three materials and a quantitative discussion on each.

## 2.3 Experimental set-ups

Four lengths of 100, 150, 200 and 250 mm for each diameter wire were considered for testing. Three specimens of each length were cut from the respective wire reels using an industrial bolt cutter and gave a total of 36 specimens to be tested. The as cut specimens were placed in an furnace and heated to a temperature of 100°C.

The specimens were held at this temperature for a sufficient amount of time and this ensured that all specimens were transformed to their austenitic state (Table 1 shows austenitic finish temperature of each material). All specimens were then removed from the furnace and allowed to cool to room temperature in still air ensuring that at the beginning of testing they were all in their martensitic states. A Hounsfield tensile tester was used for tensile experiments and specimens were clamped in such a way that the effective gauge lengths were 60, 110, 160 and 210

| Diameter (mm) | Chemical composition | | | | | Temper | Surface | Active $A_f$ (°C) |
|---|---|---|---|---|---|---|---|---|
| | Ni | Ti | C | O | Total all others | | | |
| 1 | 55.32 | 44.67 | ≤0.05 | ≤0.05 | 0.20 | Straight annealed | Oxide | 60.7 |
| 2 | 55.38 | 44.62 | ≤0.05 | ≤0.05 | ≤0.20 | Straight annealed | Oxide | 60.5 |
| 3 | 55.32 | Bal | ≤0.05 | ≤0.05 | ≤0.30 | Straight annealed | Oxide | 73 |

**Table 1** Shape memory alloy material data.
All Others Are: Al, Co, Cr, Cu, Fe, Mn, Mo, Nb, Si, W. Materials obtained from Johnson Matthey (USA).

mm. Loads were measured with 5 kN (for 1 mm diameter specimens) and 20 kN (for 2 and 3 mm diameter wires) load cells. The cross head displacement was measured by a digital encoder built in to the tensile tester. Each specimen were subjected to displacement rates of 2, 3, 4, 5, 7, 10 and 15 mm/min which gave three data sheets per length and gives a total 84 data sheets per diameter. The specimens were never fractured and after unloading they were placed back into the furnace and heated to restore their original geometric properties.

## 2.4 Quasi-plastic material responses exhibited by shape memory alloys

The quasi-plastic material response is inherent to the shape memory effect exhibited by shape memory alloys. When a load is applied to the material at low temperatures, it will deform causing an apparent plastic deformation, i.e., quasi-plasticity. This deformation is maintained until an increase in temperature causes the deformation to disappear completely. Four to 8% erasable deformations have been observed in alloys like NiTi, CuZnAl, CuAlNi, and AuCd [23, 36, 40, 41]. For a general discussion on this material response it is suggested that the reader not focus on the values for force and displacement at this stage but rather look at a qualitative description. A discussion of load vs. extension behavior for low, intermediate and high displacement rates for the different diameter wires are shown below.

## 2.5 Results and discussion

### 2.5.1 Qualitative discussion

The most observable feature of the quasi-plastic material response is the three distinct regions it shows when plotted graphically (see Figure 1A–C). For discussion purposes lets call them, respectively, the initial elastic region (IE), a nearly horizontal region (NH), and finally another elastic region (FE). All of these regions show an amount of yielding. Since regions 1 and 3 shows elastic behavior (which implies elastic properties), unloading from these regions will remove the strains obtained here. These two elastic regions suggest that the specimen changes from its initial state to some final state. Furthermore it is also seen that the slopes of these elastic curves are similar thus implying equal elastic constants. The nearly horizontal regions on these graphs thus determine the location of the transformation behavior from one elastic state to the

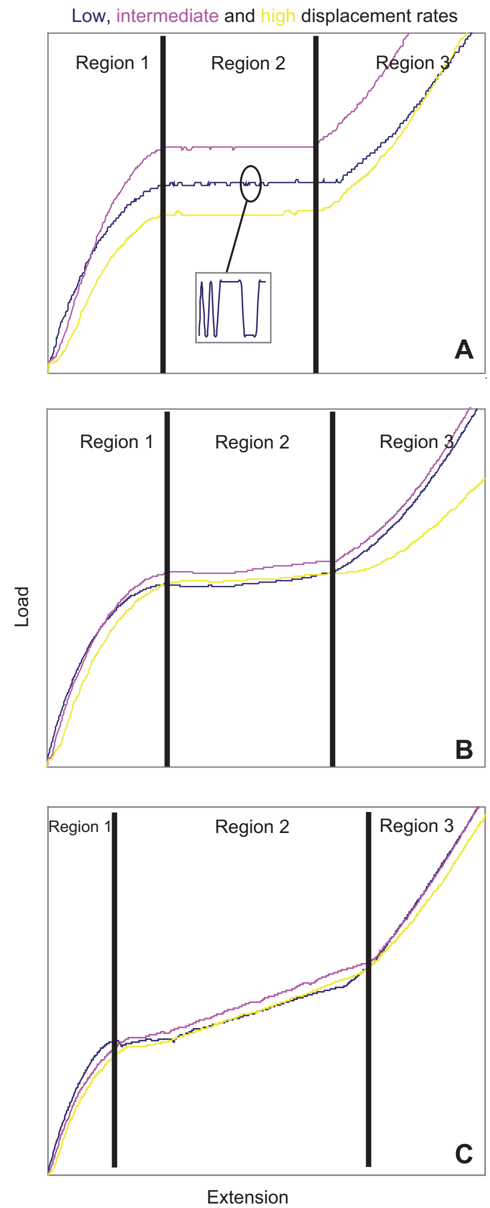


**Figure 1** Load-extension behavior for NiTi Shape memory alloy wires of (A) 1 mm, (B) 2 mm and (C) 3 mm diameters at low, intermediate and high displacement rates.

other. It also has the largest value of displacement compared to the other two regions. The end of transformation usually has a distinct point.

This is evidenced by the graphs shown in Figure 1A–C. Literature tells us that this initial state is in fact composed of different variants of martensite formed during the transformation from austenite (particularly during cooling). One explanation for this horizontal region [11] is that when these variants are subjected to an applied load only those variants sensitive to the applied load will elongate once a certain transformation load is achieved.

The sum of these variant elongations thus produces the overall or total deformation of the specimen.

Another explanation considers these variants as alternate layers or martensitic twins packed on top of each other. When a load is applied to these twins, shear loads are produced at the twin boundaries. When the shear load reaches a certain value one of the twins flip and takes the orientation of the other. This flipping or de-twinning of layers thus produces the total deformation of the specimen [36, 39].

A closer look at the transformation region for a low displacement rate (Figure 1A) of the 1 mm diameter shape memory alloy wire shows some very interesting load-displacement behavior. The insert in Figure 1A shows an exploded view of the transformation region. It shows very small fluctuations of the load with regions of constant load between them. It is now seen that the first explanation given above disqualifies itself since it does not give an explanation for these fluctuations. If we consider the second explanation given for the horizontal region, we can take these fluctuations as the load required to produce the flipping or de-twinning of the martensitic twins. This de-twinning occurs almost at constant load and thus suggests a load induced phase transformation.

Figure 1A shows a decrease in the frequency of these fluctuations with an increase in the displacement rate. This implies that at low displacement rates more of the martensitc twins transform and at high displacement rates less transform. This would then suggest that at low displacement rates greater deformation should be achieved. This is however not the case as seen in Figure 1A. High displacement rates cause lesser fluctuations with approximately the same amount of deformation indicating that higher displacement rates induce a more homogeneous deformation in the 1 mm diameter NiTi shape memory alloy wire. An explanation for this could be that at higher displacement rates certain variants of martensite undergo deformation for a longer period of time thus giving the appearance of near homogeneous deformation.

Shaw and Kyriakedis [4, 10, 11] experimentally studied propagating phase fronts of shape memory alloys. They found that increases in the displacement rate also increased the occurrence of these propagating fronts and thus produced more homogeneous deformation behavior.

The 2 and 3 mm diameter NiTi shape memory alloy wires does not show the fluctuations observed in the transformation region (see Figure 1B and C). These specimens actually show a steeper transformation region and thus imply different kind transformation behavior.

After the transformation load has been reached and transformation commences, the 1 mm diameter wire transforms from one state to the other with a seemingly perfectly plastic behavior while the 2 and 3 mm diameter wires can take the form of plasticity with isotropic or kinematic hardening. The steeper transformation region observed in the 2 and 3 mm diameter NiTi shape memory alloy wire could be ascribed to the geometric changes of the material only. Thinner wires (1 mm or less) can thus be considered as uniaxial test specimens showing the actual horizontal transformation behavior of shape memory alloys.

Thicker wires thus show a transformational behavior with hardening, which brings into play the Poisson effect as exhibited by classical steels. These kinds of constitutive approaches using the framework of plasticity-based models was followed by researchers like Shaw and Kyriakides and Bo and Lagoudas to study mostly pseudo-elastic material responses of shape memory alloys [20, 35].

Another interesting observation regarding the quasi-plastic material response is that certain displacement rates applied to different lengths of wire induce the same kind of material response (the same transformation loads, amount of deformation during transformation, and the same slopes for the initial and final elastic regions) in all three specimens tested. Examples of this material response is observed in 1 mm diameter wires of 100, 200 and 250 mm lengths at displacement rates of 2 and 15 mm/min, 2, 4 and 10 mm/min and 2 and 10 mm/min, respectively (see Figures 2 and 3). Other displacement rates simply produced different values for the material response. This would then imply that quasi-plasticity has preferred displacement rates and this kind of material response is also observed in 2 and 3 mm diameter wires.

In their experimental investigation into the behavior of the pseudo-elastic material response exhibited by shape memory alloys, Shaw and Kyriakides [4, 10, 11] found the nucleation load of transformation to be higher than that of the transformation load. This behavior was also observed for the quasi-plastic material response of 2 and 3 mm diameter wires but not for the 1 mm diameter wire. Figure 4 shows this phenomena for 2 and 3 mm diameter wire of lengths 100 and 150 mm, respectively, at a displacement rate of 2 mm/min.

This behavior also resembles the Lüders deformation found in classical engineering steels. This behavior however disappears with an increase in the displacement rate for certain lengths of wire. Figure 5 shows the load-extension behavior of three 2 mm diameter wires of length 100 mm at a displacement rate of 7 mm/min. This behavior occurs only in one specimen and it is interesting

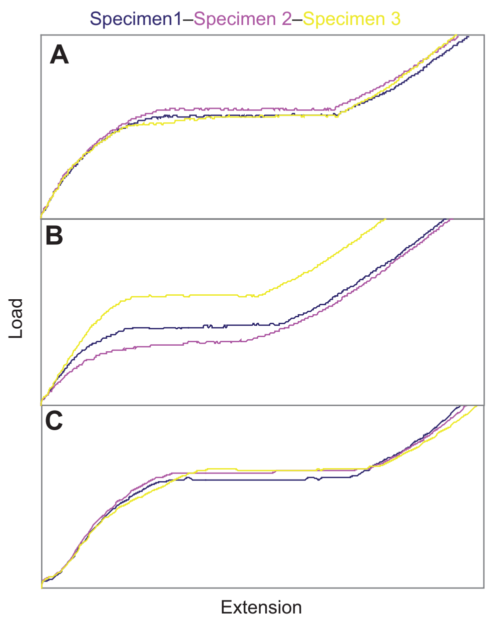


**Figure 2** Effect of displacement rate on 1 mm diameter wire of length 100 mm. (A) 2 mm/min, (B) 4 mm/min and (c) 15 mm/min.

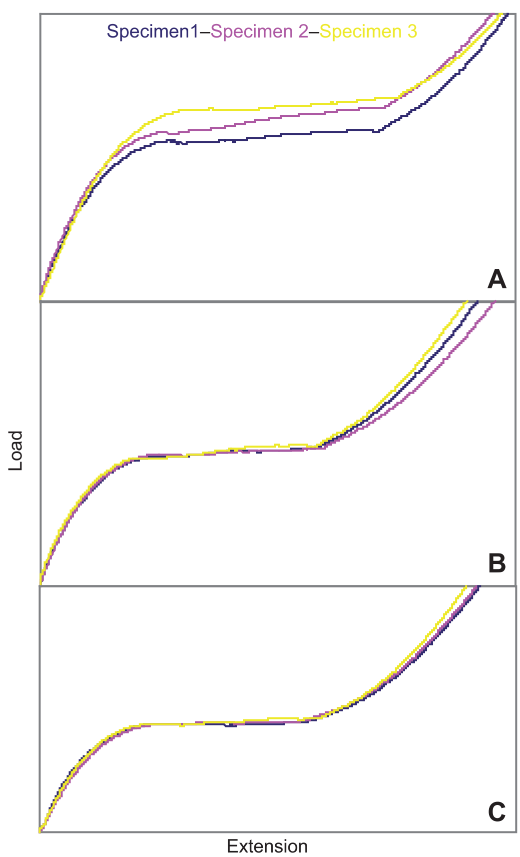


**Figure 3** Effect of displacement rate on 2 mm diameter wire of length 250 mm. (A) 2 mm/min, (B) 4 mm/min and (C) 10 mm/min.

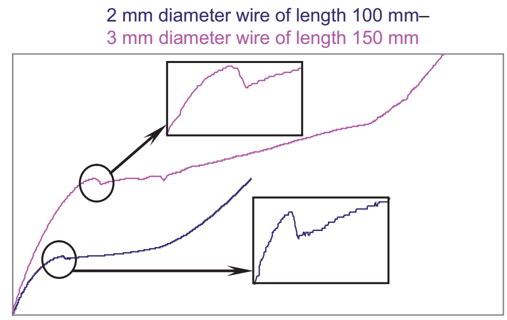


**Figure 4** Quasi-plastic material response showing relation between nucleation and transformation load behavior at a displacement rate of 2 mm/min.

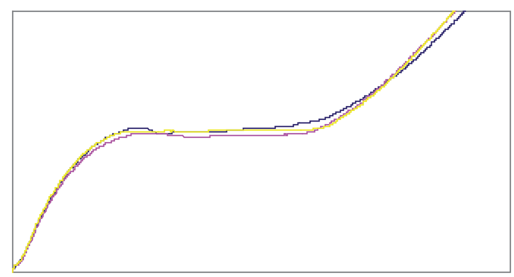

**Figure 5** Three 2 mm diameter specimens of length 100 mm each subjected to a displacement rate of 7 mm/min.

to note that when specimens behave in this way the transformation region becomes steeper showing hardening-like behavior. This observation was made for most of the 3 mm diameter wire (see Figure 6) and also for certain 2 mm diameter specimens.

### 2.5.2 Quantitative discussion

Experiments were performed to find the effect of displacement rates on geometric properties (diameter and length) and mechanical properties (initial and second yield stress,

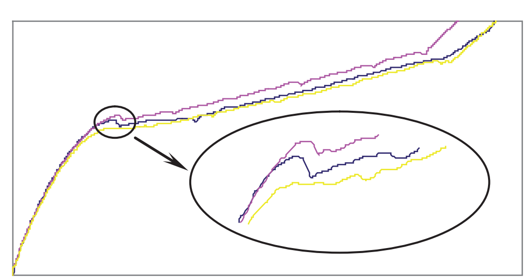

**Figure 6** Three 3 mm diameter specimens of length 150 mm each subjected to a displacement rate of 2 mm/min.

total transformation strain) of the NiTi shape memory alloy wire specimens. Exponential functions were extrapolated from the averaged data obtained from the experiments to establish the trend of quasi-plastic material responses for the three different wire diameters that was tested.

Figure 7A, B and C show the relationship between the total transformation strain and the different displacement rates that the specimens were subjected to. The trend lines indicate that an increase in the displacement rate had no effect on the total transformation strain for the 1 mm diameter wire specimens but showed slight decreases for the 2 and 3 mm diameter wires. Figure 8A, B and C show a slight decrease in the value of the initial yield stress of the different wire specimens as the displacement rate is increased.

Increases in the specimen length show a decrease in the value for the initial yield stresses for the 1 and 2 mm diameter wire specimens (see Figure 9A and B). This

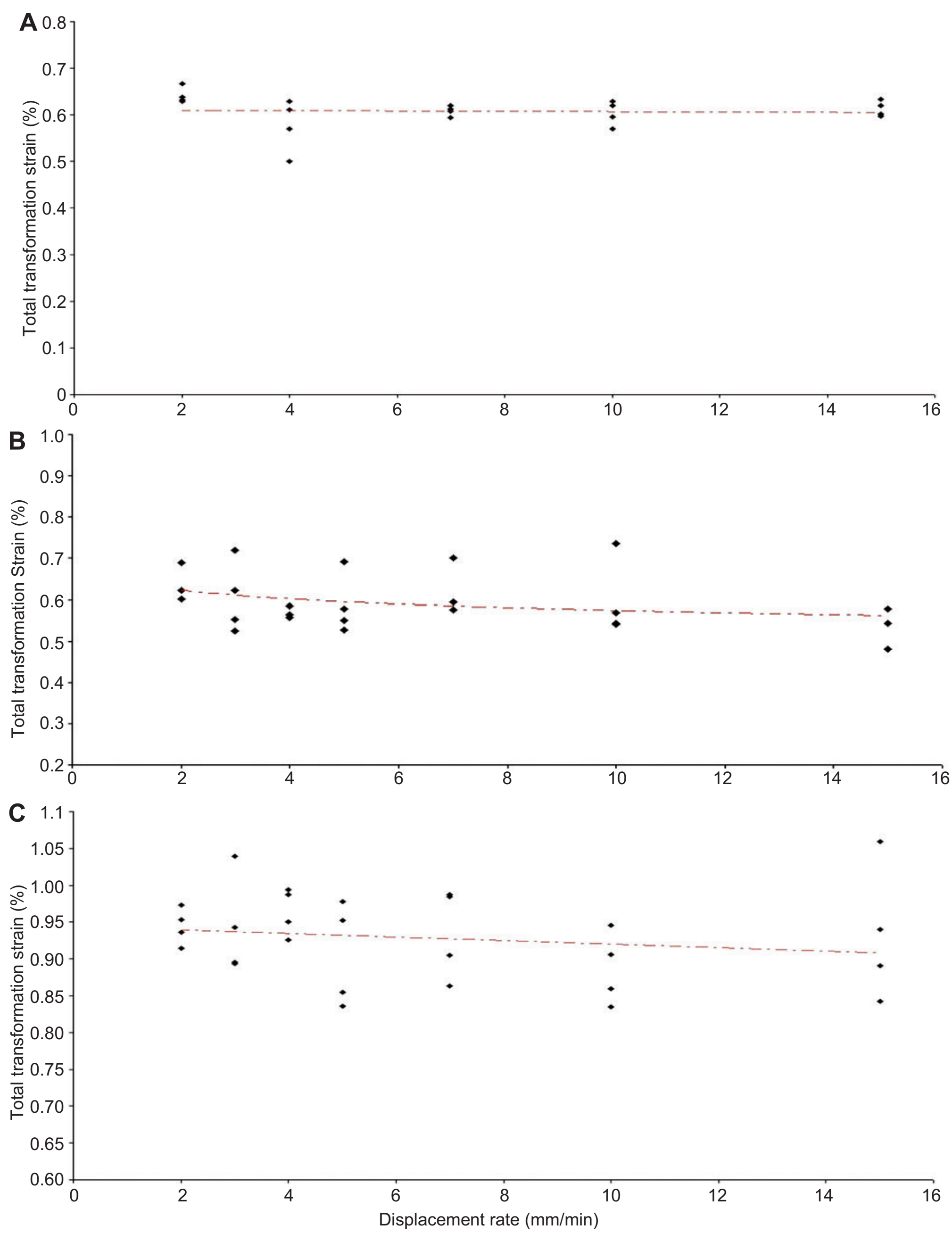


**Figure 7** Effect of displacement rate on the total transformation strain for (A) 1 mm, (B) 2 mm and (c) 3 mm diameter wire.

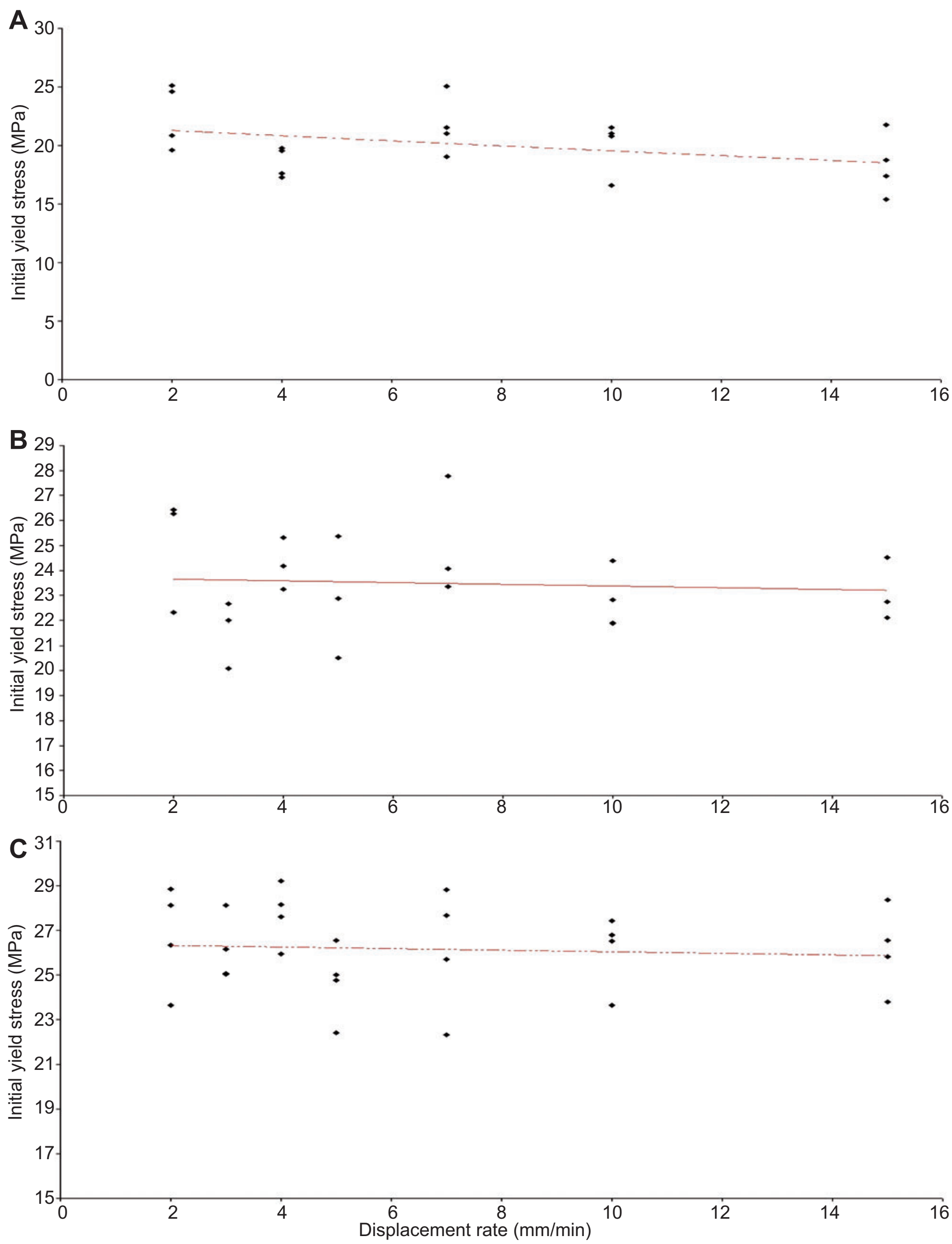


**Figure 8** Effect of displacement rate on initial yield stress for (A) 1 mm, (B) 2 mm and (C) 3 mm diameter NiTi shape memory alloy wire.

would then suggest that longer wires of these diameters yield easier than shorter wires. For a 1 mm diameter wire however, the value of the second yield stress increases with the increase in specimen length and thus compensates for the drop in initial yield stress (see Figure 9A). This behavior then maintains the total amount of transformation strain that the 1 mm diameter specimens produce.

The 2 mm diameter wire specimens exhibit a different behavior for the second yield stress (see Figure 9B) compared to that of the 1 mm diameter wire specimens. Although this trend line shows a decrease in the value of the second yield with increasing specimen length, it is not as declivitous as the initial yield stress trend line. This could then validate the slight decrease in the total transformation strain as seen in Figure 7B for the 2 mm diameter wire specimen.

Both trend lines for the initial and second yield stress values for the 3 mm diameter wire specimens show an increase with increasing specimen length. The trend line showing the behavior of the second yield stress is however steeper than that of the trend line for the initial yield stress

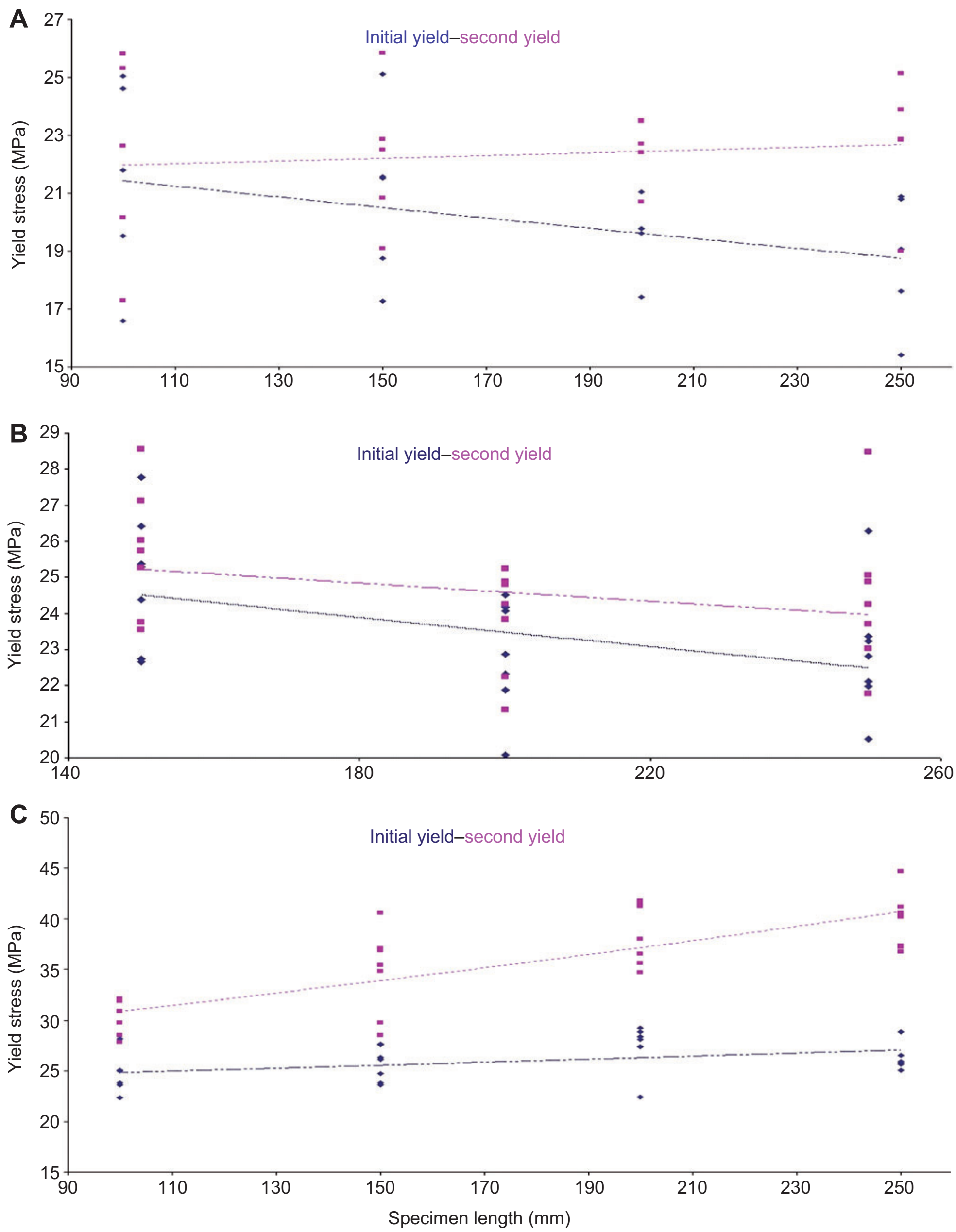


**Figure 9** Effect of specimen length on initial and second yield stresses for (A) 1 mm, (B) 2 mm and (C) 3 mm diameter NiTi shape memory alloy wire.

and almost resembles the behavior of the 1 mm diameter wire. We can then conclude that this is the way that the 3 mm wire specimens are trying to maintain the amount of transformation strain that these wires produce. The slope of the initial yield stress trend line would then suggest a decrease in the total transformation strain and this is indeed the case as seen in Figure 7C.

Figure 10A, B and C show trend lines for difference in yield stress values (second yield – initial yield) with respect to increasing specimen length. These trend lines show a parabolic increase and we can thus conclude that this is the way in which the material tries to maintain the total transformation strain that the wire specimens exhibit.

### 2.5.3 Summary of experimental findings

The experimental investigation was performed to determine the effect that different displacement rates have on

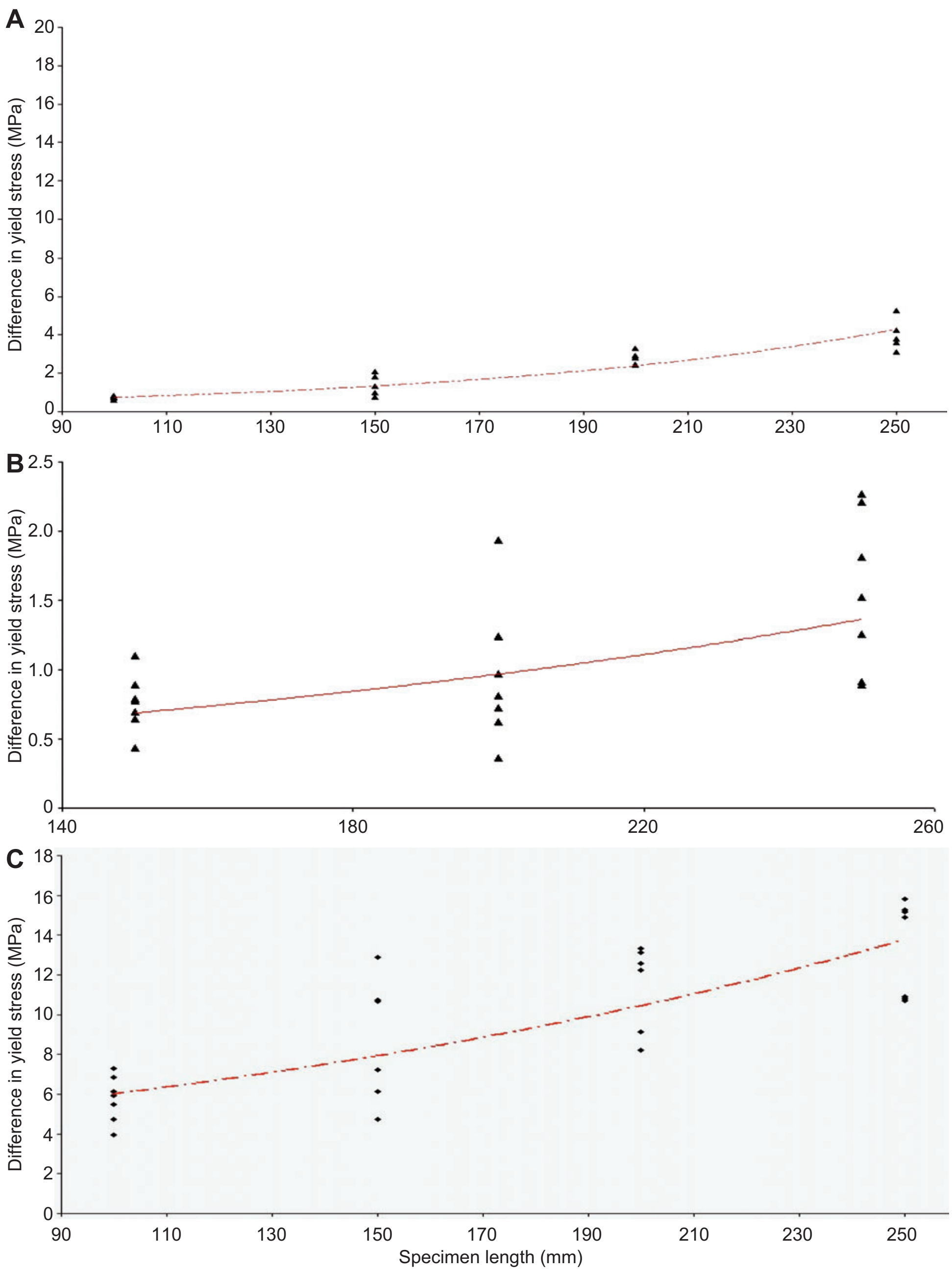


**Figure 10** Effect of specimen length on the difference in yield stress for (A) 1 mm, (B) 2 mm and (C) 3 mm diameter NiTi shape memory alloys wire.

geometric and mechanical properties of 1, 2 and 3 mm diameter NiTi shape memory alloys wires specimens of varying lengths. A summary of these findings will now follow.

- Quasi-plastic material response displays three distinct regions when plotted graphically, i.e., an initial elastic region (IE), a nearly horizontal region (NH), and finally another elastic region (FE).
- Elastic regions suggest that the specimen changes from its initial state to some final state through a transformation and the slopes of these elastic regions are similar.
- The nearly horizontal regions on these graphs thus determine the location of the transformation behavior from one elastic state to the other.
- Transformation region of the 1 mm diameter shape memory alloy wire specimens shows very small fluctuations of the load with regions of constant load between them. These load fluctuations can be regarded as the flipping or de-twinning of the martensitic twins.

- Increase in the displacement rate causes a decrease in the frequency of these fluctuations and thus produce a more homogeneous deformation.
- The 2 and 3 mm diameter NiTi shape memory alloy wires does not show the fluctuations observed in the transformation region and show a steeper transformation region.
- 1 mm diameter wire transforms from one state to the other with a seemingly perfectly plastic behavior while the 2 and 3 mm diameter wires can take the form of plasticity models that exhibit hardening behaviors.
- The steeper transformation region observed in the 2 and 3 mm diameter NiTi shape memory alloy wire could be ascribed to the geometric changes of the material only.
- Thinner wires (1 mm or less) can thus be considered as uniaxial test specimens showing the actual horizontal transformation behavior of shape memory alloys.
- Thicker wires thus show a transformational behavior with hardening-like behavior.
- Quasi-plasticity has preferred displacement rates.
- For quasi-plasticity, the nucleation load of transformation is higher than that of the transformation load.
- Lüders-like deformation was observed but disappears with an increase in the displacement rate for certain lengths of wire.
- Increase in the displacement rate had no effect on the total transformation strain for the 1 mm diameter wire specimens but showed slight decreases for the 2 and 3 mm diameter wires.
- Decreases in the value of the initial yield stress of the different wire specimens as the displacement rate is increased.
- The difference in yield stress values (second yield – initial yield) indicates the way in which the material tries to maintain the total transformation strain that the wire specimens produce.

# 3 Constitutive model for shape memory alloy line actuators

## 3.1 Introduction

This section describes the multi-well or triple well constitutive approach to simulate the complex material response, i.e., the shape memory effect and the pseudoelastic effect, exhibited by shape memory alloy materials. The idea behind this particular shape memory alloy model was originally developed by Achenbach and Müller and Achenbach and was then further refined by Müller and Seelecke and Seelecke and Kastner [36, 40, 41]. The model finds its footing firmly in the foundations of thermodynamics and statistical thermodynamics. The model is particularly appropriate to study the case of a shape memory alloy element subjected to uniaxial loading conditions. The model assumes the existence of an austenitic phase fraction and describes the evolution of two martensitic phase fractions based on the theory of thermally activated processes. What follows is a brief overview gathered from [33, 36, 39–41] of the steps followed to formulate this comprehensible uniquely powerful constitutive approach to simulate the complex material responses exhibited by shape memory alloys.

Under uniaxial loading conditions, three different metallurgical phases can be observed in a shape memory alloy material body. The constitutive approach takes these phases to be the austenite phase $A$ and two martensitic twin variants $M_{\pm}$ (see Figure 11). In order to construct a model for the line actuator as a whole, the lattice particles are arranged in layers to form a stack of N such layers thus representing a single crystal tensile specimen. The layers are arranged at an angle, $\theta$, to the direction of the tensile load according to the crystallographic axes of the specimen (see Figure 12). This angle is chosen as $45^0$ so that the layers experience the maximum shear load. On the left of Figure 12 we see the body at low temperature, in the martensitic state. It has alternating layers of the two martensitic variants, $M_+$ and $M_-$ at 50% each.

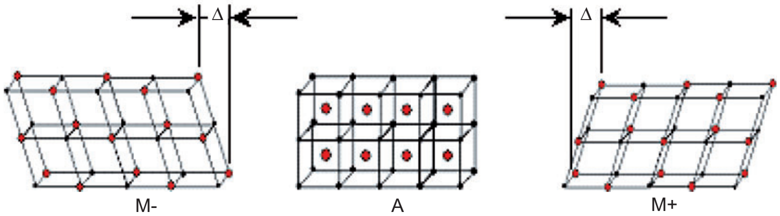


**Figure 11** Three configuration of a shape memory alloy lattice particle ($M_+$, $M_-$ and A).

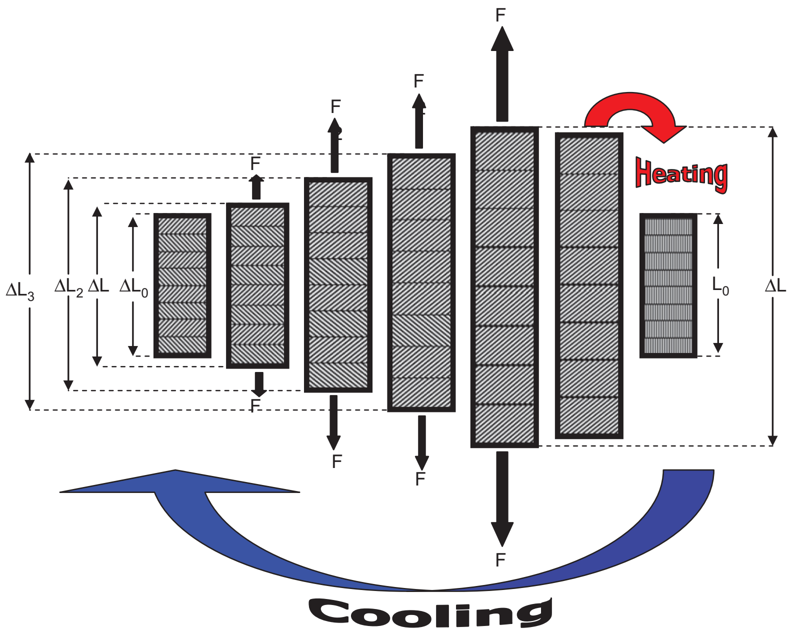


**Figure 12** Layer structure of macroscopic shape memory alloy model.

This defines the natural state of the body that has an original length of $L_0$. The application of a tensile load will subject the layers to a shear load. As seen in Figure 12, the $M_+$ layers become flatter while the $M_-$ layers will become steeper. The vertical component of the shear lengths, $\frac{\Delta_i}{\sqrt{2}}$ (summed over all $N$ layers) will provide the total deformation of the body and is given by

$$D = L - L_0 = \frac{1}{\sqrt{2}} \sum_{\Delta} \Delta N_{\Delta}, \qquad (1)$$

$N_\Delta$ is the number of layers with the shear length Δ and the summation extends over all possible shear lengths. Unloading lets the specimen fall back to the natural state so that a small deformation is elastic. If the load is increased however, there comes a point where the $M_-$ layers will flip over and become $M_+$ layers (see Figure 12 at load $F_2$). The flipped layers provide a large shear length and consequently, the deformation increases drastically. Upon subsequent unloading, the layers settle into the $M_+$ minimum so that a large deformation remains.

Figure 13 is a schematic representation of the load vs. deformation behavior of the shape memory alloy layers. It is considered that while the specimen is loaded between 0 and $F_1$, its behavior is still purely elastic. As $F_2$ is reached however, the layers are preparing to flip. $F_2$ thus represents our yield load and flipping or de-twinning as we shall call it from now on, commences at this constant load. This is also the region where we observe the greatest deformation. The region between 0 and $F_1$ signifies the initial elastic region and $F_2$ the initial yield stress. It is noted that not all the layers flip at once but instead go one after the other. This then simulates the inhomogeneous deformation during the transformation region as observed in the experimental investigation of section 2.

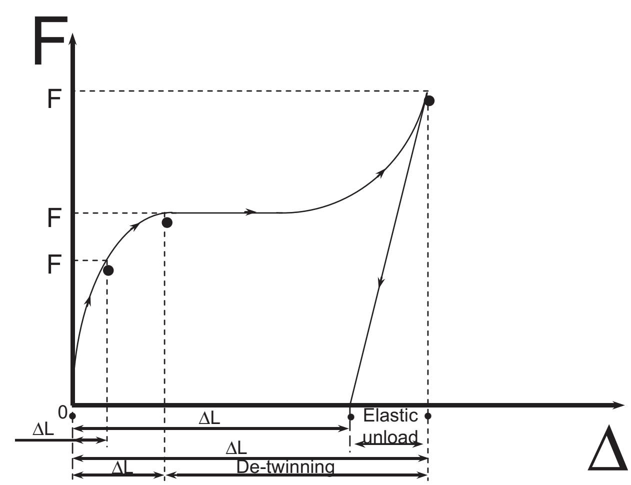


**Figure 13** Schematic representation of the quasi-plastic material response exhibited by shape memory alloys.

When all the $M_-$ layers have de-twinned to $M_+$ we see a linear relationship of the load versus deformation behavior of the $M_+$ layers. Unloading from this point, $F_3$, shows some degree of elastic unloading and the deformation that remains appear to be plastic. The behavior described above is purely mechanical and subsequent heating will cause a phase transformation to the austenitic phase and the lattice layers straighten up and accordingly the specimen contracts to its original length. This is seen on the far right hand side of Figure 12. At this point the specimen has the outward shape of the natural state, but internally it is different (more symmetric/ordered austenitic phase). The internal and external shape recovery is completed by a cooling phase where at a certain point the austenite becomes unstable and the layers revert back to their martensitic state having equal proportions of $M_+$ and $M_-$ that the specimen started out with, i.e., the original zig-zag internal structure of alternating martensitic variants. This then simulates the shape memory effect exhibited by shape memory alloys.

The assumption made in the modeling of the unique material behavior is that the phase transformations of layers are a thermally activated process. The shear length $\Delta$ of the layers fluctuates due to thermal activation, and the layers move in an energy landscape with load- and temperature-dependent barriers.

The relevant effective potential energy for a given layer is given by the Gibbs free energy, $\hat{\phi}$, or in the absence of load, by the Helmholtz free energy, $\hat{\psi}$. These are non-convex functions of the shear length with potential wells representing each of the phases. Figure 14A–C shows the Helmholtz free energy of a single lattice layer at three different temperatures.

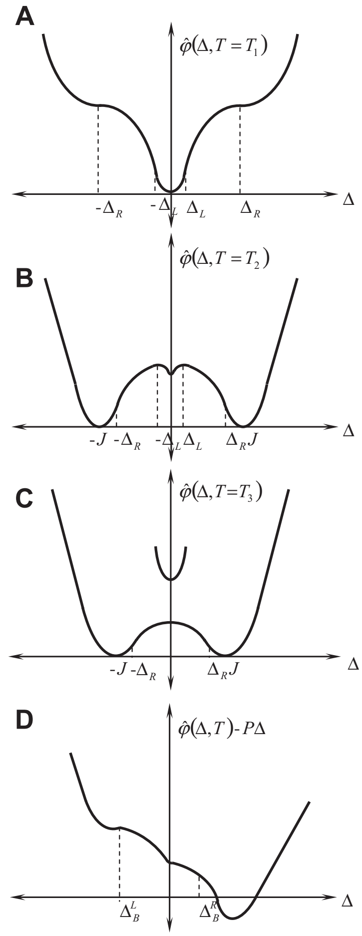


**Figure 14** Helmholtz free energy for a lattice layer at three different temperatures: (A) high, (B) intermediate and (C) low. (D) represents the gibbs free energy of a load at an intermediate temperature.

## 3.2 Phase transition of the model

Phase transitions in the model is governed by the rate laws for the phase fractions $\xi_{M_+}$, $\xi_A$ and is given by

$$\dot{\xi}_{M_-} = -\overset{-A}{\rho}\xi_{M_-} + \overset{A-}{\rho}\xi_A \tag{2}$$

and

$$\dot{\xi}_{M_+} = -\overset{+A}{\rho}\xi_{M_+} + \overset{A+}{\rho}\xi_A \tag{3}$$

under the constraint $1=\xi_{M_+}+\xi_{M_-}+\xi_A$. For a typical transformation, the rate of change of $\xi_{M_-}$ consists of a loss, due to layers that jump from $M_-$ to $A$, and a gain due to layers that jump in the reverse direction. The number of jumps are proportional to the phase fractions in the phase of origin.

The quantities $\overset{\alpha\beta}{\rho}$ in (2) and (3) are the transition probabilities from phase $\alpha$ to phase $\beta$ and are calculated using statistical thermodynamics. They are determined by the Boltzman factor corresponding to $\hat{\psi}(\Delta_B, T)$-$P\Delta_B$ where $\Delta_B$ are shear lengths at the barriers of the effective potential energy (see Figure 14D). These quantities may then be given as

$$\overset{-A}{\rho} = \frac{1}{\tau}\frac{e^{-\frac{\hat{\psi}\left(\Delta_B^L, T\right)-P\Delta_B^L}{kT}}}{\sum_{\Delta\in M_-} e^{-\frac{\hat{\psi}(\Delta, T)-P\Delta}{kT}}} \tag{4}$$

or

$$\overset{A+}{\rho} = \frac{1}{\tau}\frac{e^{-\frac{\hat{\psi}\left(\Delta_B^R, T\right)-P\Delta_B^R}{kT}}}{\sum_{\Delta\in M_-} e^{-\frac{\hat{\psi}(\Delta, T)-P\Delta}{kT}}} \tag{5}$$

so that, for example, $\overset{-A}{\rho}$ is proportional to the fraction of $M_-$ layers that have the energy of the left barrier. The probabilities $\overset{A+}{\rho}$, and $\overset{A-}{\rho}$, $\overset{+A}{\rho}$ are constructed in the same way with obvious changes appropriate to the different phases of origin and different barriers. The idea behind (4) and (5) is that once a layer has the energy of the barrier, it may pass over it. The relaxation time of this process is denoted by τ, and needs to be adjusted to yield rate of recovery rate as observed in an experiment. $T$ represents the temperature of the model body and initially we will assume it to be a constant.

The system of ordinary differential equations in time (2) and (3) permits the calculation of phase fractions for a given initial conditions provided the temperature, loading condition, and environmental temperature are known. The total specific deformation of the body is given by the sum of deformation of all the layers [derived from (1)] and is given by

$$d=\xi_A d_A+\xi_{M_+} d_{M_+}+\xi_{M_-} d_{M_-} \qquad (6)$$

Eq. (6) can also be considered the load-deformation relation which is complemented by the system of non-linear ordinary differential equations for the martensitic phase fractions. This section is concluded with initial numerical simulations to illustrate the models capability to reproduce the quasi-plastic material response exhibited by shape memory alloy specimens observed in the experimental investigation of section 2 (see Figure 15A). Since the model assumes an equal amount of martensitic variants (50% of each) as an initial condition, Figure 15B shows the evolution of the phase transformation as the given load is applied. It shows how the $M_+$ variant increases to 100% and the $M_-$ variant decreases to 0%.

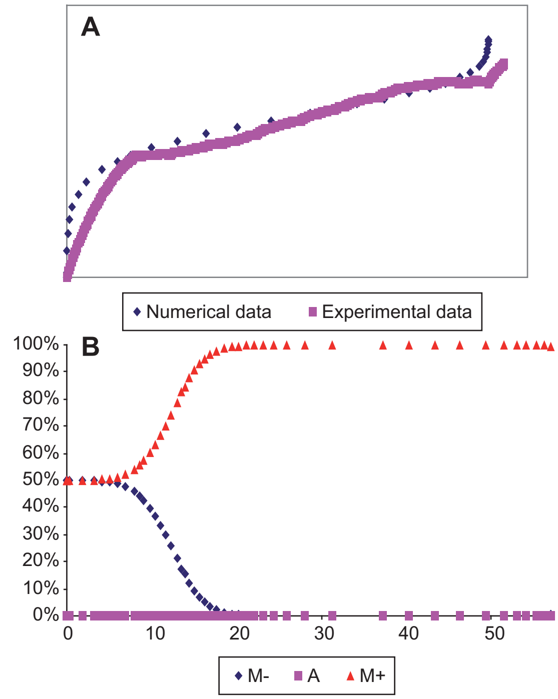


**Figure 15** (A) Mechanical load cycle of a NiTi shape memory alloy wire specimen of 3 mm diameter and length 200 mm showing numerical fit. (B) Numerical interpretation of load induced martensitic phase transformation during quasi-plastic material response.

# 4 Research projects currently undertaken

## 4.1 The conceptualization and design of a smart prosthetic limb

Because of the social nature of human beings and the need to always feel accepted in a group, it is important for those with physical disabilities to appear the same as those in the group that they are socializing with. To this end it is of utmost importance for prosthetic limbs to appear as natural as possible. Recent developments in SMA research and due to their unique characteristics, robotic technology can now be used to improve even more current prosthetic devices and thus enhance the quality of life of the physically disabled. In comparison with hydraulic, pneumatic or electric actuator systems the shape memory systems are distinguished by small weight, small space requirement, simple construction, large stroke and force production.

The aim of this research project is to conceptualise, design and manufacture a prosthetic hand that will mimic the human hand more efficiently. A network of artificial muscles comprising of shape memory wires will provide actuation for this prosthetic limb. The development of this prosthetic limb is done in collaboration with an academic partner, Mr. M. Riddles (Technical Manager, Rapid Prototyping Centre, Faculty of Engineering, Cape Peninsula University of Technology).

## 4.2 The conceptualization and design of a smart conveyor system

This project intends to redesign the entire take-up or belt tensioning system of a conveyor system by incorporating shape memory alloy wires for smart actuation. Furthermore we intend to develop smart rollers to ensure that tracking of the belt is always true. These two developments will save time on tensioning of belts at start-up of a new conveyor system as well as during belt replacements. Fiber optic technology will also be incorporated into this system to obtain and maintain the correct tension in the conveyor belt. This research is done in collaboration with a local industrial partner, Mr. D. Millar (Project Manager, Arcrite Engineering situated in Cape Town's Airport Industrial Area) and an academic partner, Mr. M. Riddles.

### 4.3 The conceptualization, design and prototyping of a smart aileron for increased maneuverability of aircraft

The shape, structure and movements of a bird's wing create an ideal situation for flight. The ranges of motion of the wing give the bird its remarkable maneuverability. The flight of a conventional fixed wing aircraft has to a certain extent mimicked some of the manoeuvrability of a bird. This maneuverability is due to hinged flaps, spoilers and ailerons found on aircraft wings.

The operation of these components causes acute angles to be formed between them and the wing during flying. Fluid mechanics courses have shown that this causes separation of the fluid molecules flowing over the wing. The aim of this research project is to incorporate a smart material into a wing and thus make it a smart structure. We will attempt to eliminate the hinged aileron by just activating the tip of the wing to create more efficient movements.

### 4.4 The conceptualisation, design and prototyping of a shape memory engine

Conventional engines use fossil fuel for their operation. Apart from the role of the by-products of these fossil fuels contributing to pollution, it is also a non-renewable source of energy. The aim of this research project is to develop a smart engine or "green engine" using shape memory alloys. It is envisaged that the engine will harness the shape memory effect for its operation.

### 4.5 The conceptualization, design and prototyping of a smart self-aligning system

Solar cells absorb the maximum amount of energy when the panels are positioned perpendicularly to the sun's rays. Conventional methods of installation for solar panels only allows for a short period of maximum energy absorption. This is due to the movement of the earth and the panel being fixed in one position. The aim of this project is to develop a self-aligning platform that will be activated by shape memory alloys thus making it a smart structure. It is envisaged that this platform will automatically adjust itself to the position of the sun and thus allow for maximum energy absorption of solar cells located on it.

## 5 Conclusions

An experimental investigation into the quasi-plastic material response exhibited by NiTi shape memory alloy wires of 1, 2 and 3 mm diameter was conducted. The results obtained were consistent with what other researchers found in the area of shape memory alloy research. It shows in particular that the displacement rate has no effect on the amount of uniaxial transformation strain produced by the shape memory alloy materials. These results will no doubt help in the design of the research projects currently undertaken at the Smart Alignment Research Group.

The multi-well constitutive approach used for the simulation of the quasi-plastic material response shows good quantitative agreement with the experimental findings of section 2 and thus validates its use in this capacity. The constitutive model will now be used in a finite element formulation to assist in the design of smart or intelligent structures specifically suited for actuation and/or sensing purposes.

**Acknowledgements:** The authors wish to thank to the National Research Foundation (GUN NO. 2064979) for their financial support given to this research project.

## References

[1] Roger CA. *Sci. Am.* 1995, 154–157.
[2] Chopra I. *Smart Structures and Materials 1996: Smart Structures and Integrated Systems. Proc. SPIE 2717.* Chorpa I, Ed. SPIE: Bellingham, WA, 1996, 20–62.
[3] Brei D. *Smart Structures for Automotive Applications Using Novel Materials*. Internal report. Department of Mechanical Engineering, University of Michigan: Ann Arbor, MI, 2002.
[4] Shaw JA, Kyriakides S. *J. Mech. Phys. Solids*. 1995, 43, 1243–1281.

[5] Van Hambeeck J. *Mater. Sci. Eng.* 1999, A273–275, 134–148.
[6] Huang W. *Acta Mater.* 1999, 47, 2769–2776.
[7] Lagoudas DC, Garner LJ, Rediniotis OK, Wilson N. *Modeling and Experiments of the Hysteretic Response of an Active Hydrofoil Actuated by SMA Line Actuators.* Internal publication. Aerospace Engineering Department, Texas A&M University: College Station, TX.
[8] Miller DA, Lagoudas DC. *Mater. Sci. Eng. A.* 2001, 308, 161–175.
[9] Shaw JA. *Int. J. Solids Struct.* 2002, 39, 1275–1305.
[10] Shaw JA, Kyriakides S. *Acta Mater.* 1997, 45, 683–700.
[11] Shaw JA, Kyriakides S. *Int. J. Plasticity* 1998, 13, 837–871.
[12] Boyd JG, Lagoudas DC. *Int. J. Plasticity* 1996, 12, 805–842.
[13] Lu ZK, Weng GJ. *J. Mech. Phys. Solids.* 1997, 45, 1905–1928.
[14] Otsuka K, Shimizu K. *Proc. Int. Conf. Solid-Solid Phase Transformations*, Pittsburgh, 1981.
[15] Bhattacharyya K. *Theory of Martensitic Microstructure and the Shape Memory Effect*. Internal publication. Division of Engineering and Applied Science, 104–44, California Institute of Technology: Pasadena, CA 91125, USA.
[16] Lagoudas DC, Bo Z. *Smart Mater, Struct.* 1994, 3, 309–317.
[17] Sawada T, Tobushi H, Kimura K, Hattori T, Tanaka K, Lin P. *JSME Int. J. Series A* 1993, 36, 395–401.
[18] Brocca M, Brinson LC, Bazant ZP. *J. Mech. Phys. Solids* 2002, 50, 1051–1077.
[19] Qidwai MA, Lagoudas DC. *Int. J. Plasticity* 2000, 16, 1309–1343.
[20] Delaey L, Krishnan RV, Tas H, Warldmont H. Thermoelasticity, pseudoelasticity and the memory effects associated with martensitic transformations, *J. Mater. Sci*. 1974, 9.
[21] Shaw JA. *Int. J. Plasticity* 2000, 16, 541–652.
[22] Webb GV, Kurdila AJ, Lagoudas DC. *J. Intell. Mater. Syst. Struct.* 1998, 9, 432–448.
[23] Govindjee S, Hall GJ. *Int. J. Solids Struct.* 2000, 37, 735–760.
[24] Qidwai MA, Lagoudas DC. *J. Numer. Meth. Engng.* 1999, 47, 1123–1168.
[25] Shu SG, Lagoudas DC, Hughes D, Wen JT. *Smart Mater. Struct.* 1997, 6, 265–277.
[26] Zhu J, Liang N, Huang W, Liew KM, Liu Z. *Int. J. Solids Struct.* 2002, 39, 741–763.
[27] Chen WC, QuiPing W, Kang JH, Winfree NA. *Int. J. Solids Struct.* 2001, 38, 8989–8998.
[28] Fukuda T, Kakeshita T, Houjoh H, Shiraishi S, Saburi T. *Mater. Sci. Eng.* 1999, A273–A275, 166–169.
[29] Liu Y, Xie ZL, Van Hambeeck J, Delaey L. *Acta Mater.* 1999, 47, 645–660.
[30] Lu TJ, Hutchinson JW, Evans AG. *J. Mech. Phys. Solids.* 2001, 49, 2071–2093.
[31] Schetky L. McD. Shape-Memory Alloys, Academic, New York, 1979, 241, p. 68.
[32] Auricchio F, Sacco E. *Int. J. Solids Struct.* 2001, 38, 6123–6145.
[33] Huo Y. *On the Thermodynamics of Pseudoelasticity*. Thesis submitted towards the degree of Dr.-Ing., Technical University of Berlin, 1993.
[34] Huo Y, Müller I. *Cont. Mech. Thermodyn.* 1993, 5, 163–204.
[35] Lagoudas DC, Bo Z, Qidwai MA. *Compos. Mater. Struct.* 1996, 3, 153–179.
[36] Seelecke S, Müller I. *SMA Actuators in Smart Structures*. Internal publication. Institut für Verfahrenstechnik, Technical University of Berlin, Sekr. HF2, Straβe des 17 Juni 135, D-10623 Berlin, 2000.
[37] Faciu C, Mihailescu-Suliciu M. *Int. J. Solids Struct.* 2002, 39, 3811–3830.
[38] Ohta T. *Mater. Sci. Eng., A.* 2001, 312, 57–65.
[39] Müller I, Seelecke S. *Math. Comp. Model.* 34, Preprint 38. Peragon Press: Oxford, New Yark, 2001.
[40] Seelecke S, Büskens C. *Proceedings of the OPTI 97, Computer Aided Optimum Design of Structures,* Hernàndez S, Brebbia CA, Eds., Comp. Mech. Press: Rome, Italy, September 8–10, 1997.
[41] Seelecke S. *FE Simulation and Optimal Control of Adaptive Beams Using SMA Wires.* Internal publication. Berlin: Institut für Verfahrenstechnik, Technical University of Berlin, Sekr. HF2, Straβe des 17 Juni 135, D-10623 Berlin, 1997.